

CHAPTER 1

Introduction :

The scientific study of sedimentary rocks and the processes that create them, known as sedimentology, offers vital information on tectonic histories and historical environmental conditions. The continuous convergence of the Indian and Eurasian plates in the Himalayan foreland basin has produced a dynamic depositional environment where active tectonics and river systems interact.

This interaction of sedimentation and deformation is documented by the Middle to Upper Siwalik Group strata exposed by the Mohand Rao River section, which is close to Mohand village in Saharanpur District, Uttar Pradesh.

Objective :

- Create a thorough lithostratigraphic framework that highlights important facies, such as coal-bearing overbank deposits, multistorey sandstone and siltstone, and oligomicitic Para conglomerates.
- Record sedimentary features, such as load castings, ascending ripples, cross-bedding, and flame structures—that document soft-sediment deformation and paleo-flow dynamics.
- Use a clinometer to obtain accurate structural data (strike, dip, apparent and true thickness). GPS and compass for tectonic interpretation and stratigraphic correction.
- To clarify sediment transport mechanisms and facies linkages, combine quantitative models (stream power equation) with fundamental concepts (Law of Superposition, Original Horizontality, and Walther's Law).

Through these studies we also want to understand the paleo environment of Siwalik's. Key Objectives- Understand the Sedimentary Environment, Study Sedimentary Rock by Grain Size, colour, lithology, Study Sedimentary structures

CHAPTER 2

Area of Study

The basin, which is located in northern India, is a perfect place for sedimentological research since it provides a distinctive fusion of ancient sedimentary deposits and contemporary geological processes.

2.1. Geographic and Physiographic Setting:

The Mohand Rao River transect extends roughly one kilometer along the southern bank of the Mohand Rao River, centred near Mohand village ($30^{\circ}10'N$, $77^{\circ}55'E$ to $30^{\circ}13'N$, $77^{\circ}54'E$). The study area lies at elevations between 300m and 360m above mean sea level within a subtropical monsoonal climate that produces pronounced seasonal fluctuations in river discharge and sediment flux. Steeply incised channels alternate with uplifted paleo-terraces, providing diverse, accessible outcrops for sedimentological logging.

2.2. Ancient Sedimentary Deposits:

Beyond the current activities, the Mohand basin provides a window into the geological past by storing old sedimentary deposits. Sedimentary rock layers that have developed over millennia contain hints about previous tectonic events, depositional processes, and environmental conditions. Researchers can precisely reconstruct paleoenvironments and decipher the region's complex history by examining these sedimentary strata.

2.3 Tectonic Setting :

North-south convergence between the Main Boundary Thrust and Himalayan Frontal Thrust raised the Mohand anticline, a notable antiform about 80 km long and 15 km wide. Up to several kilometres of Siwalik strata were excavated during the Miocene–Pliocene due to thrust-related folding. Stepped terraces and gully structures that maintain both depositional and deformational histories were produced by this tectonic activity. The Siwalik sequence here preserves the interplay of sediment supply from the rising Himalayas and syn-orogenic deformation, making it an ideal site for understanding basin inversion processes and foreland-basin dynamics.

2.4 Terraces and Sedimentary Record :

Terraces, which were formed over geologic time by the erosive action of rivers, are one of the Mohand basin's most notable features. By providing a cross-sectional picture of depositional environments from proximal to distal, these terraces offer unique glimpses of the sedimentary record. By researching the composition, structure, and stratigraphy of these terraces, researchers can comprehend the evolution of the landscape and the interplay of geological processes throughout history.

CHAPTER 3

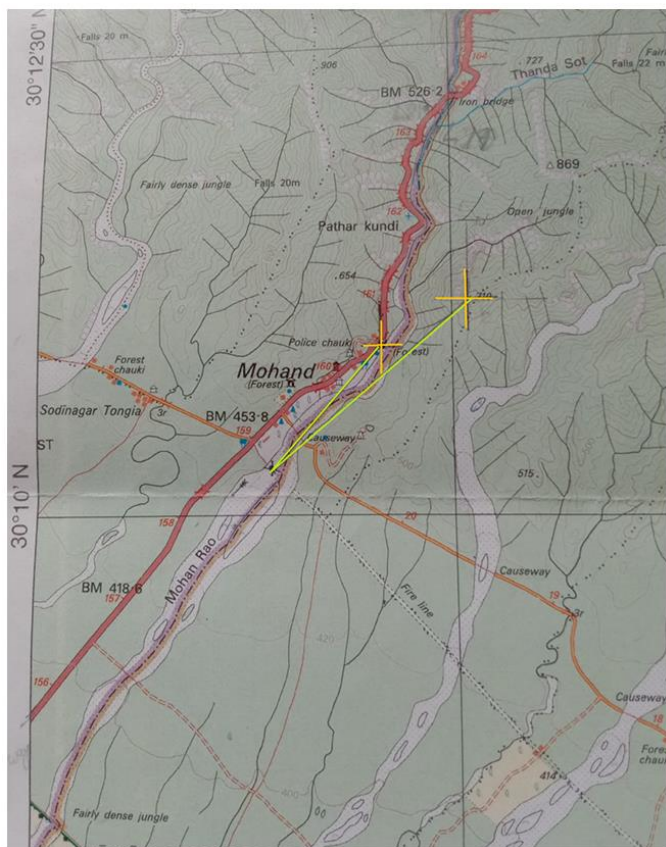
Field Data Collection , Methodology and Field activities

3.1 Methods used in Fields

a) Identification of location using topo-sheet and clinometer

Compass and photography

Accessible outcrops along a kilometer or more of the Mohand Rao River bank, from the Terrace Conglomerate Site upstream to the Forest Office downstream, were the main focus of the fieldwork. The original site number label that was noted during fieldwork was used to refer to each locality. Each site's latitude and longitude were acquired using handheld GPS units with an accuracy of ± 5 meters. In order to confirm our location on topographic maps, we used a two-point triangulation technique with a clinometer compass: toposheets were used to trace the back-bearings to two different landmarks, which intersected at our GPS location.



b) Calculation of Mean Strike and Dip (Manual + Stereonet app)



Determine strike:

- Align compass's horizontal edge with bedding plane.
- Note magnetic azimuth to ascertain bed's strike.

Measure dip:

- Rotate compass 90 degrees.
- Place compass perpendicular to strike angle in dip direction.
- Read inclination to determine dip.

Measure apparent thickness:

- Use measuring tape along exposed bed surface to record apparent thickness.

Calculate true thickness:

- Apply trigonometric adjustment: multiply apparent thickness by cosine of dip angle.

True bed thicknesses were calculated from field-measured apparent thicknesses and dip angles using the relation:

$$\text{True Thickness} = \text{Apparent Thickness} \times \cos(\text{Dip Angle})$$

Example at Site 2a:

- P1: $T_{\text{apparent}} = 69\text{cm}$, $\theta_{\text{dip}} = 10^\circ$ $T_{\text{true}} = 69 \times \cos(10^\circ) \approx 67.9\text{cm}$
- P2: $T_{\text{apparent}} = 172\text{cm}$, $\theta_{\text{dip}} = 10^\circ$ $T_{\text{true}} = 172 \times \cos(10^\circ) \approx 169.3\text{cm}$

- P3: $T_{\text{apparent}} = 64\text{cm}$, $\theta_{\text{dip}} = 15^\circ$ $T_{\text{true}} = 64 \times \cos(15^\circ) \approx 61.8\text{cm}$

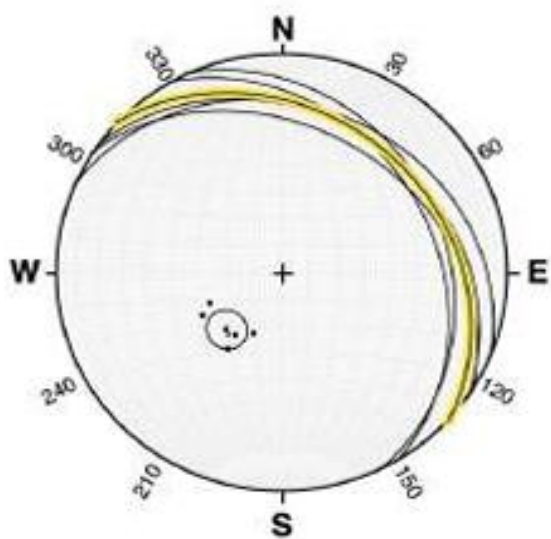
These corrections allow consistent inter-site stratigraphic correlation.

Ensure accuracy:

- Take 2–3 readings per bed to minimize errors from uneven surfaces or weathered outcrops.

We use the following procedure to calculate mean dip and strike using the Stereonet app:

1. Input the data of a sing location in the stereonet app.
2. Find the poles of all the planes entered.
3. Find the mean pole of the entered pole using (Ctrl + M) command.
4. Create a new line using the trend and Plunge Obtained of the mean pole.
5. Find the polar to the Mean pole. That plane will represent the mean dip and strike



c) Sediment Sampling and Logging

Representative samples of each lithology—ranging from oligomictic par conglomerate to fine siltstone—were collected in labelled bags. Field logs recorded: Lithology and grain size (e.g., medium sand, coarse gravel) ,Hardness (soft, mid, hard) , Color (e.g., buff sandstone, grey siltstone, red-stained marl)

,Sedimentary structures (cross-beds, ripples, load casts) , Contacts (erosional, conformable, wavy).

d) Cementation and Diagenesis Tests

Used 0.5N HCl acid to identify carbonate cementation levels in different beds. Compared top and bottom beds for reactivity, hardness, and compaction to assess diagenetic variation.

e) Structural and Tectonic Interpretation

Field Data Colle Fracture systems, soft sediment deformation features, and concordant and discordant bedding planes were noted.

used features like terrace deposits, onlaps, and channel truncations to interpret the effects of active tectonics. identified and charted paleoseismic markers, including load castings, ball-and-pillow structures, and convoluted laminae.

4.1 Field Activities

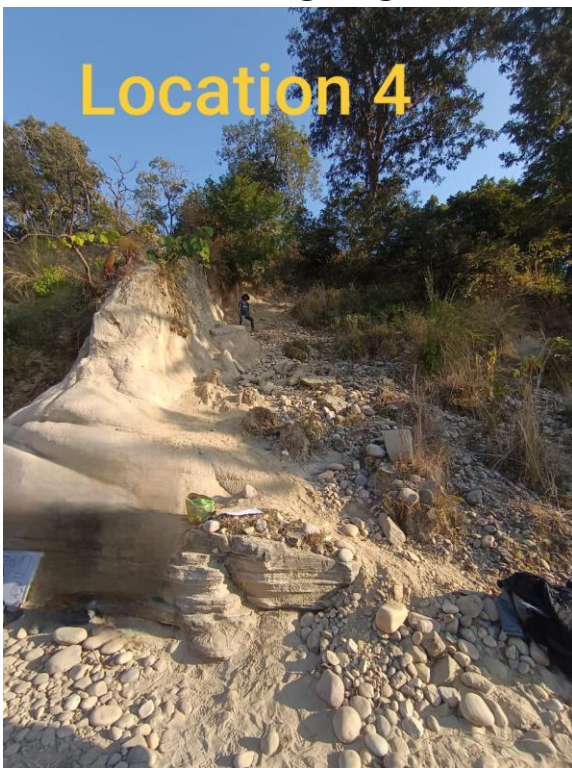
- L-2 (30°10'30"N, 77°54'80"E) Lower bed is inclined with respect to horizontal and made of sand deposition only. Laminations visible in the beds. Upper bed is made of gravel.



- L-4 (30°10'31.0"N, 77°54'20.2"E) Stacking of cross-stratified sandstone. Cross-stratification towards dip direction. Sharp erosional contact at the top, following the bedding plane.



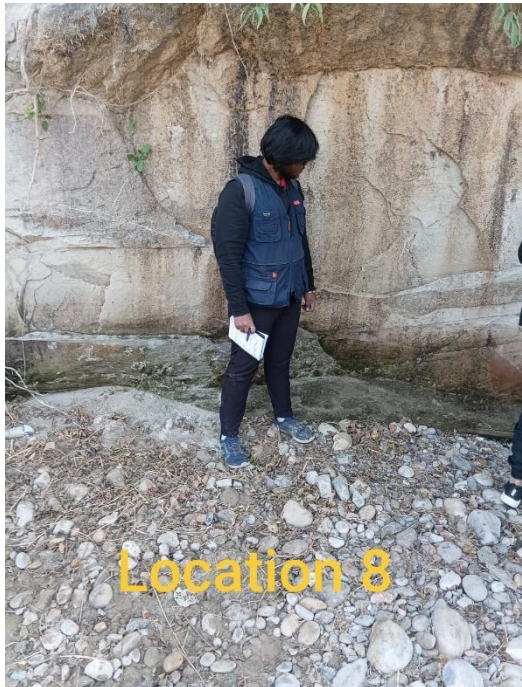
- L-5 (30°10'26"N, 77°54'15"E) We focused on analyzing ancient foreland basin stratigraphy through modern analogs. We observed Steno's law of horizontality (all sedimentary layers deposit horizontally) and the law of superposition (older rocks at bottom, younger at top). We distinguished between matrix-supported and clast-supported deposits, and noted how inclination indicates post-depositional processes. We examined the difference between dip sections (where river flow is along dip direction, creating multiple beds) and strike sections (where river flow is along strike direction, creating single beds extending over large areas).



- L-7($30^{\circ}10'52''N$, $77^{\circ}54'40''E$) We measured the strike and dip several times at Location 7, averaging about 45° for the strike and 33° for the dip. With slanted foresets and sub-contact with the upper limiting surface, the upper bed showed tabular structure. We noticed that the base had undetectable tangential contact, and the younging direction—which indicates fresher deposits—pointed upward toward the steeper former side. The laminae patterns differed according to orientation; in the flow-oblique direction, they formed wedges, whereas in the flow-perpendicular direction, they were parallel to one another. We observed that straight-crested ripples are indicated by parallel patterns. The lee side was the one that was preserved, and the upper bounding surface displayed sub-erosional features, suggesting sub-critical stratification that climbed in the direction of the dip. Brown material between laminae was identified as mud clasts— intraformational clasts that originated from floodplains within the basin. While examining the relationship between migration velocity and sediment rate, we noted thresholds for sediment preservation **where $\beta < \alpha$ results in partial preservation, $\beta \ll \alpha$ yields no preservation, and $\beta > \alpha$ produces complete preservation.** There was clear evidence of extensive trough cross-stratification, with some tapering ends creating festoon cross-stratification. While the top area had primarily planar structures, the bottom section had more troughs. The average foreset measures were 45° dip and 38° strike. The discovered laminae were not parallel but rather cut across bedding planes, with carbonates that had dissolved and precipitated on weak discordant planes. This allowed us to discriminate between concordant (syndeposition) and discordant (post-depositional) characteristics.



- L-8 to 10 (30°18'14"N, 77°91'17"E to 30°18'18"N, 77°91'12"E) We saw a channel at Location 8 that had a concave upward look as a result of lateral channel migration across a sandy basin. Multi-story sandstone complexes were created by stacking several sandstones. Acute angle truncation of the channel forming onlap, toplap in the top layer, and bottomlap in the bottom layer are among the truncation patterns that we found. The presence of a river channel was indicated by the onlap on both sides, while the deeper, thicker sedimentary sections marked the thalweg, or deepest section of the channel. Identification of flow characteristics was aided by the channel margins' discordant relationships with the underlying sand. Four stacked channels that were mostly made of fine to medium-grained sand were counted; coarser grains were mainly found close to the high-energy thalweg regions.



L-12(30°11'13"N, 77°54'45"E) Convoluted laminations, consolidated and water-saturated. Tightly folded. Mud and Iron Oxide enriched. Deformed laminae and paleo-seismic indicators present. Ball-and-pillow structure noted. Syn-sedimentary deposits, folded convolution observed in this outcrop . These features serve as paleo-seismic indicators, showing how earthquake instability affected sediments before consolidation. We identified critical ripple structures with S-shaped patterns indicating $\alpha=\beta$ conditions, along with sigmoidal laminae resulting from tangential folding. Additionally, we saw ascending ripple lamination, which produces stacked foresets by placing younger ripples on top

of older ones. Additional paleoseismic markers were ball-and-pillow constructions and mud balls made from eroded mud, which revealed the locations where water escaped to create sand balls that eventually became pillows. We found supercritical flow circumstances where gravity and wind flow predominated that resulted in antidunes and anti-ripples using the Froude number relationship ($Fr = V^2/(gh)$).



- L- 13 (30°11'22"N, 77°54'50"E) We observed potholes formed by gravel movement in water, creating distinctive erosional features in bed boundaries. Both strike sections and dip sections revealed trough cross-stratification, with tangential contacts on lower boundary planes and flow direction matching the dip and younging direction.



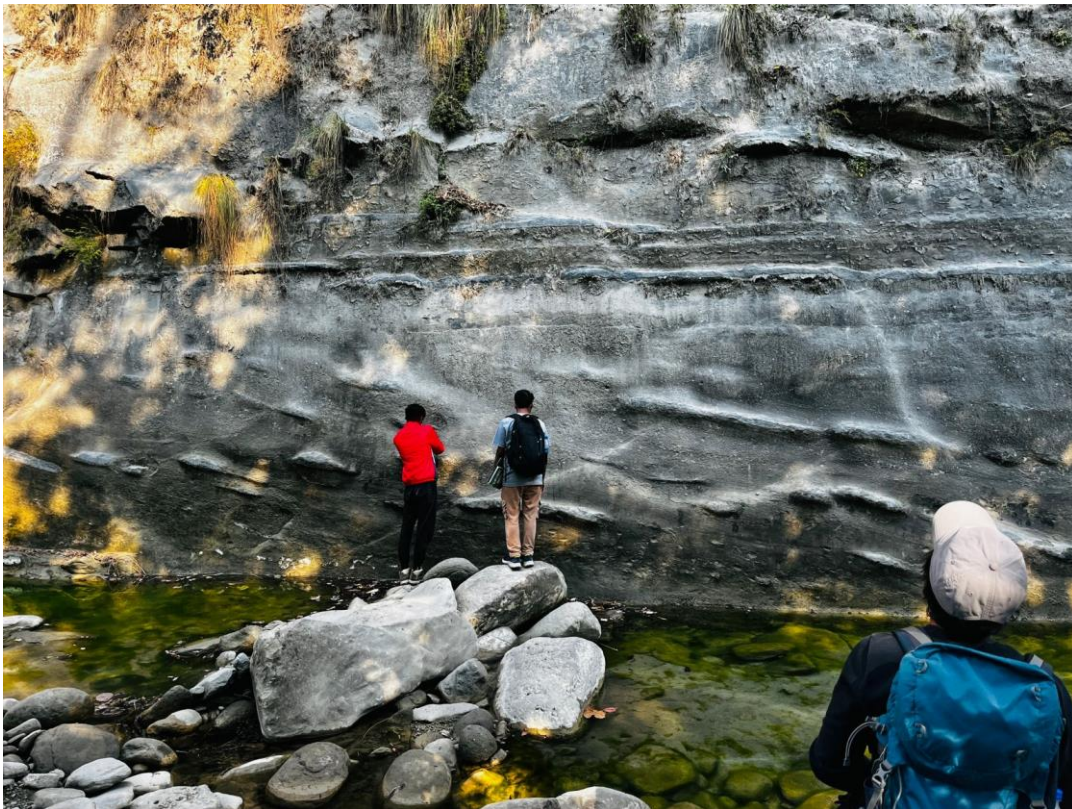
- L-14 (30°11'25"N, 77°54'52"E) One massive mudstone bed called marl has highly fissile shale. Silt to clay transition. Lower layer is mudstone without lamination, ex situ, carbonate precipitation. Colour: old sample is red colour newer deposition is grey . On other side we see Fining upward sequence (sand to silt).



- L-15(30°11'27"N, 77°54'54"E) Sulphur observes in deeper part of channel and became coal in thalweg . Sulphur act as reducing agent so reduces organic matter to coal



- L-20 ($30^{\circ}12'6''N$, $77^{\circ}54'57''E$) Large-scale trough cross-stratification. Foresets visible. Strike-parallel section. Calcite precipitated rock. Cementation: Continuous, discontinuous, and selective.



- L-21 ($30^{\circ}12'12''N$, $77^{\circ}55'1''E$) This is also a multi storey sandstone with very clear bedding plane . It has inclined structure where plane is visible in a strike section. This is a flow oblique section. Brown garnet was seen along with shiny muscovite (ice like) dark greenish amphibole was observed.



- L-22 (30°12'22"N, 77°55'3"E) Channel with sandstone and pebbles. Reddish-brown color. Poorly graded quartzite. Stoss and full lee observed. Mostly pebbles of quartzite and chert.



- L-23(30°12'37"N, 77°55'5"E) There is a top gravel + sand bed and a sandstone bed underneath . There is an unconformity in sand+ gravel bed called strath .Gravel bedded river ->continuous uplift and erosion leads to terrace formation (flat surface above is terrace treed



- L-27 (30°12'54"N, 77°55'23"E) Oligomictic paraconglomerate. Convolute structure. Red oxidized mud. Laminae are highly corrugated. Alternate dark/light bands. Gneiss clasts. Mudclasts from reworking. Gully observed.



- L-29 (30°12'57"N, 77°55'27"E) Our field methodology used a 1 m × 1 m grid sample technique at Location 28 to record the size, shape, and composition of granite, quartzite, and chert pebbles. According to source interpretation, reworked pebbles from far-off sources showed mineralogical maturity with uncommon soft rocks, and their end members were composed of granite, chert, and quartzite. The Tethyan Himalayan & South Tibetan Detachment, the SubHimalaya, the Lesser & Greater Himalaya, the earlier foreland basin deposits, and the contemporary catchment were all part of the source area hierarchy.



- L-30 ($30^{\circ}13'8''N$, $77^{\circ}55'36''E$) Outcrop W to E. Rounded pebbles indicate fluvial origin. Soul marks show direction. Load casts, gutter marks, reworked floodplain. Corrugated laminae. Flame peaks seen. Light and dark brown laminae. Seismite features.



- L-30($30^{\circ}13'3''N$, $77^{\circ}55'36''E$) Continuosu folded lamina observed . Formed due to seismic shaking and leads to water squeezing upwards and forms flame structures . Water saturated sediment gives high seismic shaking .They are paleoseismic event indicators and are called seismites Paleoseismicity increases as we gradually move up



- L-31(30°13'9"N, 77°55'40"E) Top-> Gravel bed , bottom-> conglomerate , the location was almost at GST(gravel sand transition zone) . Strata is present only in horizontal . we observed coarsening of upward sequence of rock records .



Here We also left our mark of presence

- L-32(Final Location near Tunnel)We saw a mix of rounded and angular gravel, a distributary channel pattern, a sub-aerial alluvial fan habitat, signs of a sharp slope change, and poorly sorted sediments at the final tunnel position. The alluvial fan had a feeder channel with the highest sediment deposition and a distinctive concave upward slope that set it apart from delta deposits.



CHAPTER - 4

Data Analysis

4.1 Location Id's and their Coordinates

Site ID Latitude Longitude
2a 30°10'27.4"N 77°54'03.2"E
2b 30°10'27.4"N 77°54'03.2"E
3 30°10'31.1"N 77°54'14.1"E
4a 30°10'31.0"N 77°54'20.2"E
4b 30°10'31.0"N 77°54'20.2"E
5 30°10'36"N 77°54'25"E
6 30°10'49"N 77°54'33"E
7 30°10'52"N 77°54'40"E
8 30°10'53"N 77°54'42.1"E
9 30°10'54"N 77°54'43.7"E
10 30°10'54.8"N 77°54'43.8"E
11 30°11'6"N 77°54'44"E
12 30°11'13"N 77°54'45"E
13 30°11'22"N 77°54'50"E
14 30°11'25"N 77°54'52"E
15 30°11'27"N 77°54'54"E
16 30°11'28"N 77°54'54"E
17 30°11'37"N 77°54'53"E
18 30°11'50"N 77°54'53"E

19	30°11'55"N	77°54'52"E
20	30°12'6"N	77°54'57"E
21	30°12'12"N	77°55'1"E
22	30°12'22"N	77°55'3"E
23	30°12'37"N	77°55'5"E
24	30°12'40"N	77°55'7"E
25	30°12'44"N	77°55'17"E
26	30°12'51"N	77°55'22"E
27	30°12'54"N	77°55'23"E
28	30°12'57"N	77°55'29"E
29	30°13'3"N	77°55'36"E
30	30°13'7"N	77°55'39"E
31	30°13'9"N	77°55'40"E
32	30°13'12"N	77°55'40"E

4.2 Raw Data and Averaged Data Tables

9	26	41	26. 5	39	26	44	26. 5	39	28	35	26. 6	37	26	41	
10	26	35	29	35	24	36	25	35	25	35	25	35	27	36	
11	26	35	26	35	26	35	26	35	26	35	26	35	26	35	
12	26	35	26	35	26	35	26	35	26	35	26	35	26	35	
13	26	35	26	35	26	35	26	35	26	35	26	35	26	35	
14	25	330	25	345	45	315	25	330	25	330	25	345	35	315	
15	25	317	27. 5	317	26	310	25	317	25	317	25	317	25	317	
16	25	290	25	290	25	285	25	290	25	290	25	290	25	290	
17	25	290	25	290	25	290	25	290	25	290	25	290	25	290	
18	30	298	32	287	28	304	28	297	27	317	22	300	25	290	
19	32	314	32	287	28	290	28	290	28	290	28	290	20	300	
20	31	283	30	310	33	285	31	283	31	280	30	280	32	286	
21	30	310	30	280	30	310	30	313	30	313	30	312	30	315	
22	27	310	27	210	30	310	30	313	30	313	30	312	31	315	
23	30	280	30	280	30	280	30	280	30	280	30	280	30	280	
24	30	315	31	315	30	315	27	307	30	315	30	299	27	310	
25	22	322	24	265	25	265	22	312	22	322	30	315	31	313	
26	24	265	20	320	20	310	24	263	21	315	24	315	25	270	
27	20	285	22	285	22	285	21	315	21	315	24	263	25	270	
28	26	283	26	283	26	283	22	285	22	285	22	285	22	285	

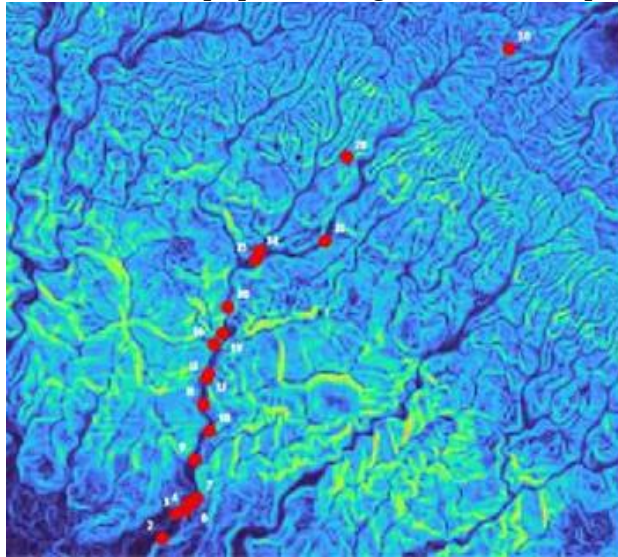
Average Data Table

Location	Average Dip (°)	Average Strike (°)
2a	11.1	41
2b	8	48.5
3	7.1	65
4a	13.9	78.3
4b	22.3	36.8
5	54.1	107.7
6	32.7	37.6
7	26	35
8	25	55
9	26.5	39.4
10	25.9	35.3
11	26	35
12	26	35
13	26	35
14	29.3	330
15	25.5	316.1
16	25	289.3

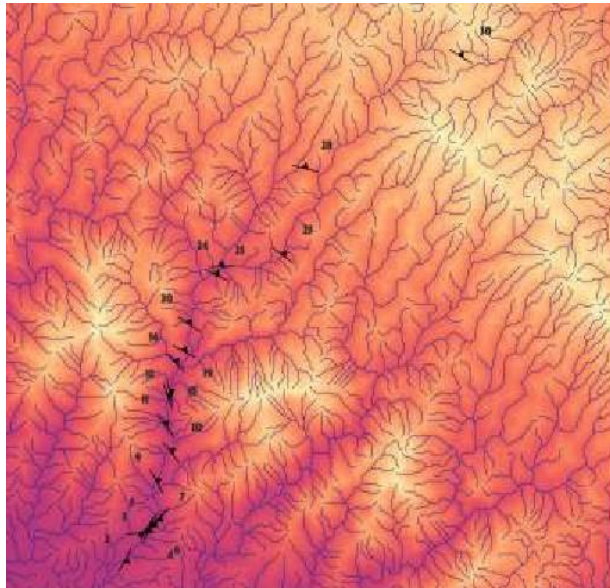
17	25	290
18	27.4	299
19	28	293
20	31.1	286.7
21	30	307.6
22	29.3	297.6
23	30	280
24	29.3	310.9

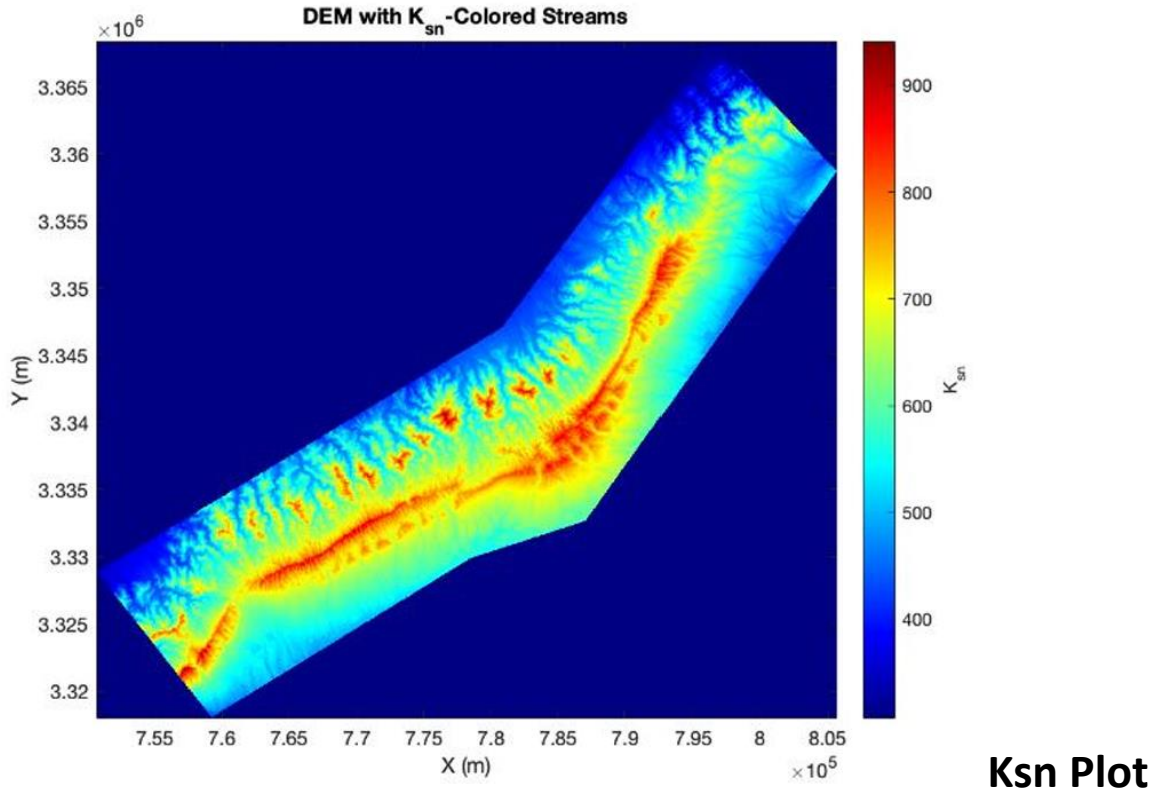
4.3 Analysis Using ArcGis(Arcmap)

We obtained DEM of our study area. We plotted our locations on the DEM. From the elevation profile, we formed the slope profile using ArcGIS. This helps us differentiate the highlands from the ground level.



We also used ArcGIS to form the channel network from the DEM after filling the sinks. We obtain precise idea about the lowlands in the area.





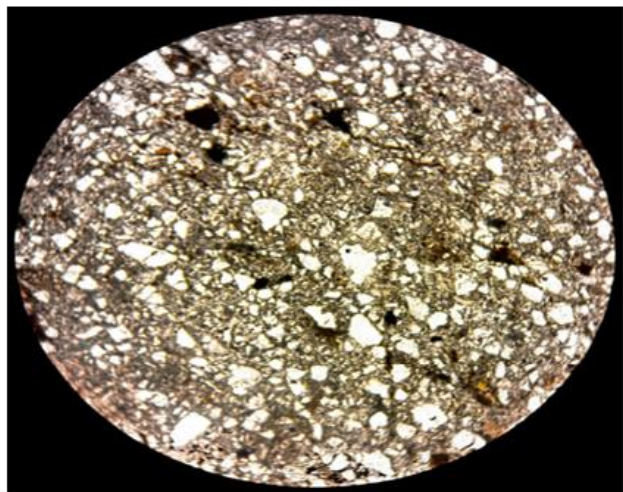
Ksn Plot

The research accurately pinpoints a number of important points:

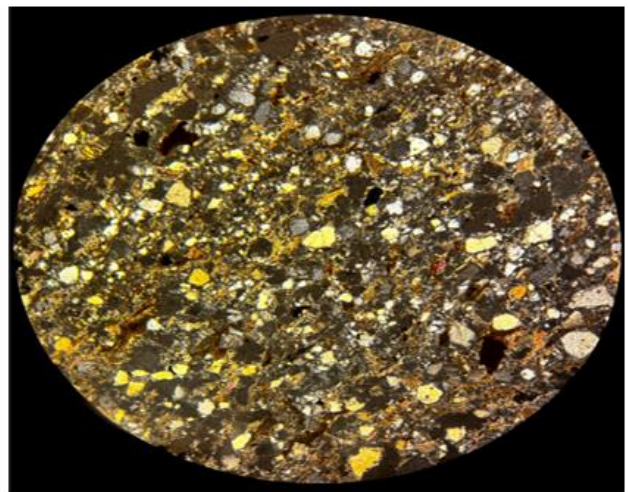
1. Prior to lithification, the sedimentary rocks were first horizontally deposited in a foreland basin.
2. These rocks have since been raised by a basin inversion process.
3. A large-scale fold structure is indicated by the shifting dip patterns.
4. In particular, the dip appears to drop away from the core and grows toward the internal portion of the range.
5. This pattern points to an antiform structure.
6. As a result of the uplift that followed, rivers were compelled to cut through the landscape, forming unique geomorphic features.

4.4 Thin Section analysis

a) Site 7



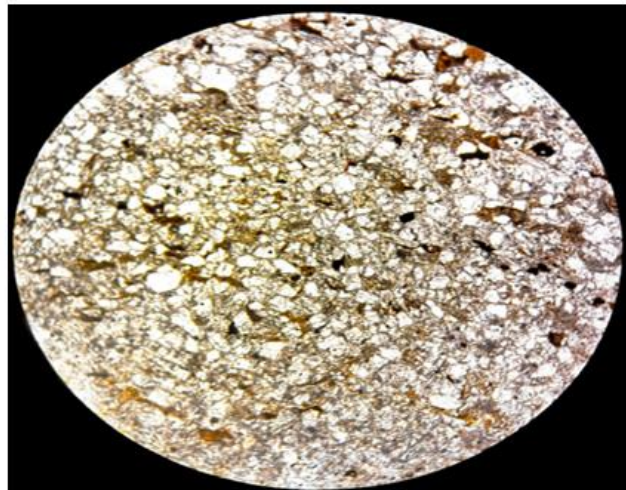
(a) Under PPL



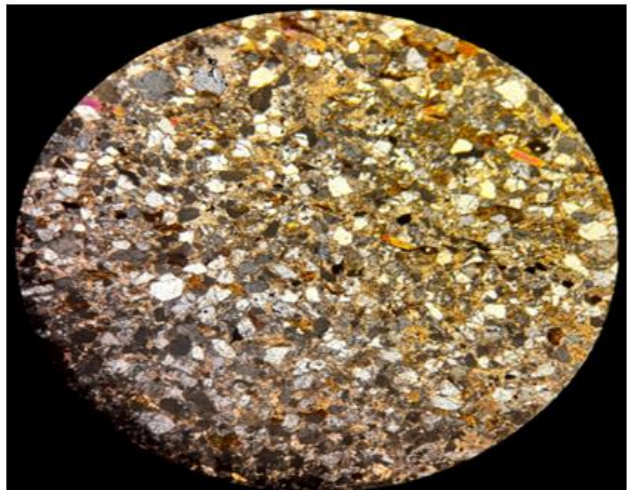
(b) Under XPL

In the thin section from Site 7, framework grains are almost entirely quartz, with minor muscovite and feldspar. Grains display moderate sorting and subangular to subrounded shapes, and abundant grain-to-grain contacts produce a clast-supported fabric. The low interstitial matrix and pore-filling cement indicates extensive burial compaction following deposition.

b) Site 13



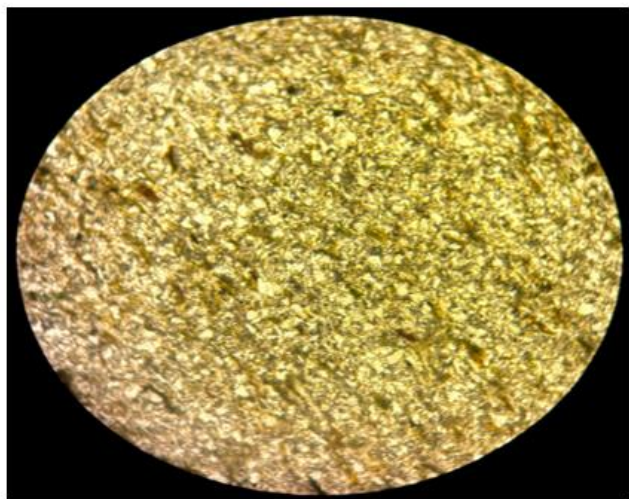
(a) Under PPL



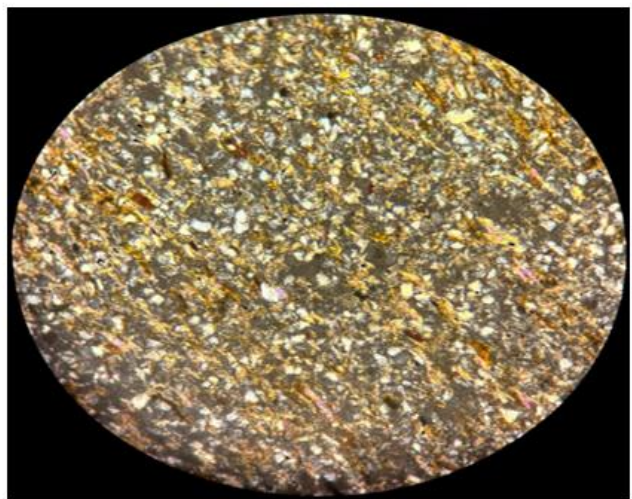
(b) Under XPL

The mineral assemblage of Site 13 consists of feldspar, biotite, quartz, muscovite, and chlorite. Here, the angular and poorly sorted grains indicate rapid deposition near a metamorphic source. Shallow burial conditions are indicated by the isolated areas of early diagenetic siliceous cement and the low level of overall compaction.

c) Site 24



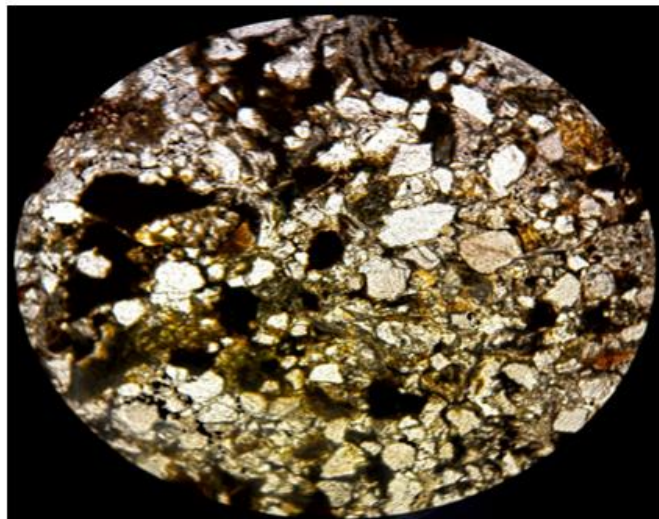
(a) Under PPL



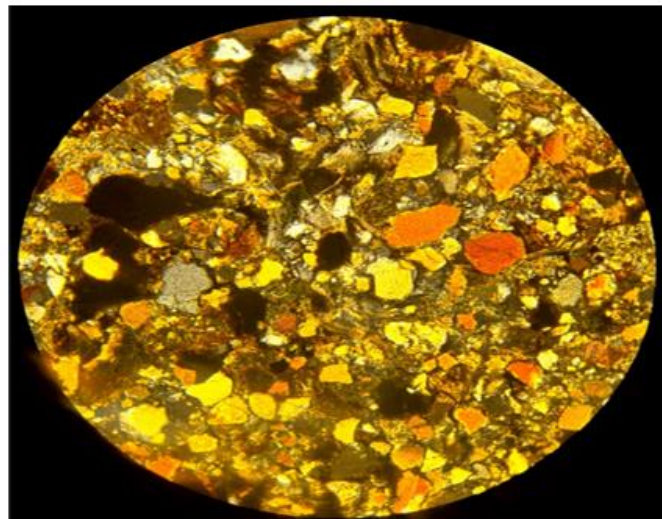
(b) Under XPL

Although the quartz, feldspar, biotite, and mica are all present in the same suite on the slide from Site 24, the rock is noticeably softer due to a larger volume of fine-grained matrix; the grain shapes are still angular to subangular, suggesting limited transport; and although silica cement binds the grains, the higher matrix content indicates less compaction than in deeper-buried units.

d) Site 27



(a) Under PPL



(b) Under XPL

Lastly, the thin piece of Site 27 has quartz intergrown with feldspar and garnet, along with trace amounts of biotite and chlorite. Significant compaction is indicated by tight, sutured connections and almost no intergranular holes, whereas modest grain rounding points to intermediate transport lengths. The presence of garnet underscores a metamorphic provenance for much of the sediment load.

Together, these petrographic observations—grain composition, shape, sorting, matrix content, and cementation—reveal a progressive change from proximal, poorly transported deposits to more deeply buried and compacted sandstones along the Mohand Rao transect. The following table presents a refined grain count analysis of selected thin sections. The percentages were derived through counting under polarized light microscopy, with each count totaling approximately 200 grains.

Site ID	Quartz (%)	Feldspar (%)	Rock Fragments (%)
7	90.21	2.12	5.88
13	89.2	6.1	5.13
24	95.41	1.37	3.22
27	94.18	1.69	4.13

CHAPTER 5

Summary

Plotting data on topographic and geological maps, measuring bedding attitudes (strike & dip), and comparing field observations with satellite imagery and DEM data are all examples of practical mapping skills.

Structural Interpretation: The presence of a large-scale antiform structure (probably caused by basin inversion) was inferred by recognizing differences in bedding dip orientation (from SW to SE).

Geomorphic Understanding: Noted how surface processes, especially river incision patterns and associated topographic expressions, are influenced by rock tilting.

Tectonic insights: Recognized how the Himalayan tectonics shaped the current Mohand Range's terrain by causing the sediments in the foreland basins to deform.

Depositional Environments: The outcrops showed a shift from low-energy overbank and floodplain deposits (siltstones, marls, and coal seams) to high-energy braided river systems (oligomictic paraconglomerates and multistory sand stones). This facies fluctuation, which reflects lateral alterations in depositional environments, is consistent with Walther's Law.

Field Observation Skills: Improved capacity to relate abstract ideas to geological structures found on the ground, including folds, river patterns, and erosion surfaces.